JTTEE5 20:234–242
DOI: 10.1007/s11666-010-9557-1
1059-9630/$19.00 © ASM International

Peer Reviewed

Influence of Impact Angle and Gas Temperature on Mechanical Properties of Titanium Cold Spray Deposits

K. Binder, J. Gottschalk, M. Kollenda, F. Gärtner, and T. Klassen

(Submitted June 1, 2010; in revised form August 27, 2010)

Titanium coatings have a high potential for various applications and can be produced in high quality by cold spraying. In this contribution, the two major challenges are addressed: (i) optimizing mechanical properties by systematic variation of process parameters, and (ii) evaluating the influence of the spray angle with respect to complex geometries. High deposition efficiencies of more than 95% can be obtained and the coatings show very low porosities as well as high tensile strength of over 450 MPa by using nitrogen as process gas. The influence of process conditions on the mechanical properties is discussed on the basis of single impact morphologies, coating microstructures, tubular coating tensile, as well as shear tests.

Keywords coating-substrate interaction, cold gas dynamic spraying, influence of spray parameters

1. Introduction

Due to the hexagonal closed packed (hcp) structure, plastic deformation of titanium (Ti) is limited and shaping processes like rolling (760-815 °C) and forging (815-900 °C) have to be performed at sufficiently high temperatures and/or require subsequent annealing steps, and all these have to be performed in inert environments (Ref 1-3). Therefore, less costly routes for processing more complex shapes are requested by industry.

Cold spraying is a promising technique for producing thick coatings with near-bulk properties. Metal particles are accelerated toward a substrate and deposited at the desired spot. Bonding of particles is facilitated by shear instabilities that occur during impact due to the plastic deformation under high strain rates (Ref 4-6). Because process temperatures (T) are comparatively low (≤1000 °C) and processing times are typically shorter than about 1 ms, contamination by interstitial impurities like oxygen or nitrogen can be minimized.

Several attempts were made to produce Ti-coatings or freestanding parts by cold spraying (Ref 7-12). Due to the limited deformability of Ti, so far costly helium had to be used to obtain sufficiently high impact velocities and plastic deformation. Only then, coatings with the requested low porosities were obtained. Using nitrogen as process gas, mostly low deposition efficiencies, quite high porosities and nonsufficient coating strengths were achieved (Ref 7-12). With recent developments in cold spraying and with the release of the Kinetiks® 8000 system, much harsher particle impact conditions can be accessed.

This study investigates cold spraying of titanium under high-end parameter sets using nitrogen as process gas. Cold spraying with gas temperatures of up to 1000 °C at a pressure of 4 MPa should result in high deposition efficiencies close to the saturation limit. For improving coating properties and to study influences on bonding, it is necessary to reach the saturation limit of the deposition efficiency (Ref 6). In particular, under particle impact conditions that by far exceed critical conditions for bonding, enhanced mechanical coating properties are expected that are similar to those of respective purity bulk titanium. Thus, a major focus of this study is given to impact conditions and the correlation to coating microstructures and mechanical properties. Moreover, with respect to the production of complex titanium parts, a detailed study on the influence of deviations from the ideal spray angle is provided. For cold spraying of copper, previous investigations demonstrated that the deposition efficiency declines with increasing deviation from perpendicular impacts (Ref 13, 14). Nevertheless, so far no correlation to coating properties was supplied.

This article is an invited paper selected from presentations at the 2010 International Thermal Spray Conference and has been expanded from the original presentation. It is simultaneously published in *Thermal Spray: Global Solutions for Future Applications, Proceedings of the 2010 International Thermal Spray Conference*, Singapore, May 3-5, 2010, Basil R. Marple, Arvind Agarwal, Margaret M. Hyland, Yuk-Chiu Lau, Chang-Jiu Li, Rogerio S. Lima, and Ghislain Montavon, Ed., ASM International, Materials Park, OH, 2011.

K. Binder, J. Gottschalk, M. Kollenda, F. Gärtner, and **T. Klassen**, Helmut Schmidt University, University of the Federal Armed Forces, Hamburg, Germany. Contact e-mail: kurt.binder@hsu-hh.de.

2. Experimental Methods

2.1 Cold Gas Spraying

In this study, commercially pure titanium powder grade 1 with a size distribution of −45 µm and a $d_{50} = 33.5$ µm was used as feedstock material. For coating production by cold spraying, the Helmut Schmidt University (HSU) prototype of the CGT Kinetiks® 8000 was operated with nitrogen as process and powder feed gas. The deposition efficiency (DE) was measured by weighing the samples before and after the coating procedure and comparing the mass gain with the powder feed mass during the coating process.

2.2 Investigation of Microstructures and Properties

To study microstructures and morphologies of the titanium powder, cross sections were prepared and analyzed by optical microscopy (OM; type: DM4000M from Leica Microsystems CMS GmbH, Mannheim, Germany). For microstructural investigations of powders and coatings as well as for determining coating porosities, polished cross sections were investigated by optical microscopy (OM; type: DM4000M from Leica Microsystems CMS GmbH, Mannheim, Germany). For image analysis with a commercial software (KS 3000 Version 3.0, Carl Zeiss Visions GmbH, Munich, Germany), high contrast levels are used to guarantee reproducible results. The porosity of each cross section was measured at four different sites, and then averaged. The oxygen content of powders and mechanically detached coatings was quantitatively measured by spectrometric methods using a commercial analyzer of the type EF 400/TC 436DR from Leco instruments, USA. Hardness measurements were performed on polished cross sections using a Vickers indenter (type Miniload from Leitz, Germany) at a load of 300 g (HV 0.3, DIN 50133).

2.3 Tubular Coating Tensile Test (TCT-Test)

To provide data about tensile strength of the coating in a fast and cost-efficient way, an own developed Tubular Coating Tensile (TCT) test was used. Two cylindrical aluminum substrates with a diameter and a length of 25 mm are fixed face to face together by a screw that also keeps them aligned on a tube like holder. The dimensions of the substrate are similar to that of bond strength samples (EN 582 or ASTM C633). To ensure that there is no gap between both cylinders, they are machined down to a diameter of 24 mm, resulting in a roughness of about 40 µm. During the coating process, the holder with the substrate is rotated by a lath with 180 rounds per minute. The traverse robot speed for spraying was set to 234 mm per minute and the spray distance was 60 mm. Typical coating thicknesses range between 500 and 1500 µm. After the coating process, the sample of this coated cylinder assembly was unscrewed from the holder and fixed in the mechanical testing equipment. Tensile testing is performed by the same set-up that is used for bond strength tests. For each parameter setting, minimum three samples are tested, as well following the requirements for bond strength tests. In evaluating results from TCT testing, it must be considered that the geometrical design of the sample leads to a stress concentration (notch effect) in the pulled coating. Locally higher stresses initiate failure at an average load stress that is lower than the tensile strength of the coating. This effect has to be considered and the measured values need to be multiplied with a factor of 1.5 to 1.7 to gain the real ultimate tensile strength of the coating, as demonstrated in previous investigation (Ref 5, 16). This correlation factor was determined by finite element analysis of the maximum stress concentration upon failure in TCT-testing (Fig. 1), and verified by correlating values obtained in TCT-tests with results of micro-flat tensile tests of identically processed samples (Ref 5). In all cases, the standard deviation was less than 10%.

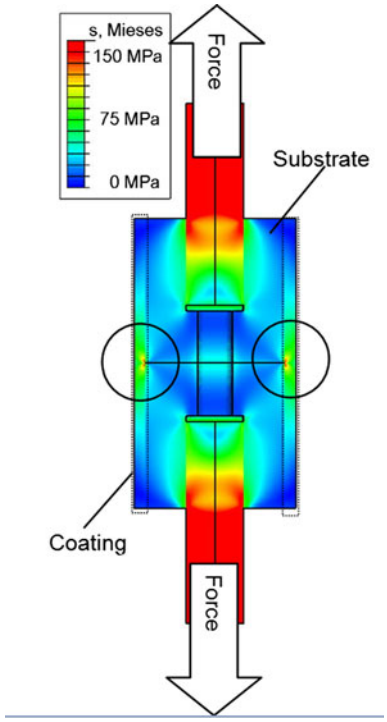

Fig. 1 Sectional view of a coated TCT sample. Stress concentration in the coating upon failure as a result from FEM modeling TCT-testing. The tensile concentration is highest (the notch effect, encircled in the figure) at the face sites of the cylinders

2.4 Shear Test

The shear test (DIN EN 15340, sketch in Fig. 2) investigates the cohesion and adhesion of the coating. In standard pull-off experiments according to DIN EN 582 or ASTM C633, a counter-body is fixed onto the surface by a polymer resin and then the assembly of substrate, coating, resin and counter-body is subjected to a tensile test. However, these tests could only supply a lower estimate for the bond strength, because a significant amount of specimens failed within the resin, representing the weakest link.

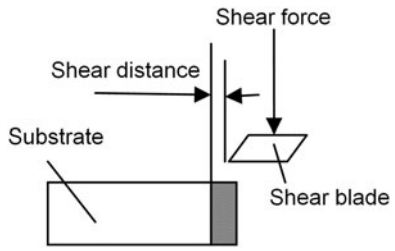

Fig. 2 Sketch demonstrating the principle of the shear test

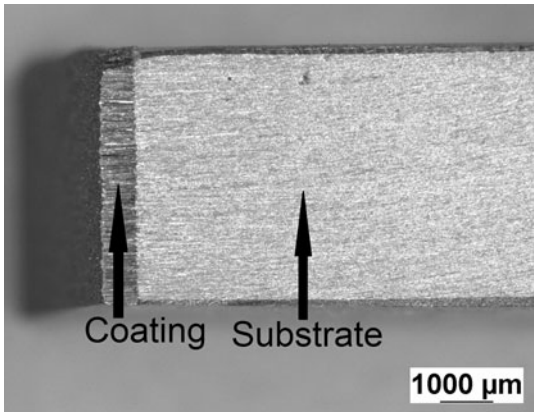

Fig. 3 Macro-images of a Ti-coated shear substrate

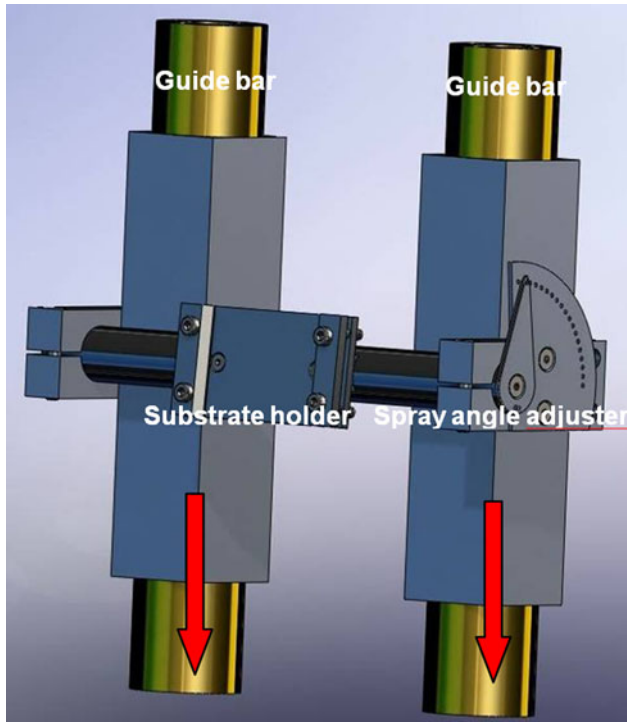

Fig. 4 Sketch for the Wipe test device. The arrows stand for the fall direction of the wipe test device. The device falls perpendicular through the spray jet

The substrates for the shear test have a brick-shaped form in the dimensions of $30 \times 10 \times 5$ mm^3 and are coated on the 10×5 mm^2 face side (Fig. 3). The low carbon steel substrates were grit blasted before spraying; the aluminum substrates were cleaned in acetone. During the coating process, six substrates separated by a thin metal plate are coated in one row. During these tests, following failure behaviors can occur: The first type results into a nearly total detachment of both parts, which can be attributed to the internal adhesion of the coating and substrate being stronger than the cohesion between both. The second type shows a discontinuous, comminuted detachment due to the cohesion between coating and substrate being much stronger than the internal adhesion. The third type describes a mixture out of type one and two. In the following, only results from the type one failure will be reported to simplify the relation to bond strength tests. In this type, the standard deviation of measured shear strengths was always below 5%.

2.5 Wipe-Tests

For investigating single impact morphologies under well-defined spray angles, a new wipe-test device was build (Fig. 4). This device should ensure that less than one monolayer of particles is deposited during a single pass through the spray jet. By gravity sliding down on guide bars from the upper position, the sample carriage with the substrate holder passed the fixed spray jet with a speed of 7 m/s. Well-defined spray angles between 0° and 90° can be adjusted in 5° steps. For studying single impacts that reveal information about flattening behavior and areas of shear instabilities (ASI), the substrates were polished prior to the wipe test. The individual particle impact morphologies were investigated by scanning electron microscopy (SEM, type XL40, Philips Electron Optics, Eindhoven, The Netherlands) under a tilt angle to obtain perspective view micrographs.

3. Results and Discussion

3.1 Powder Microstructures and Purity

Chemical analysis reveals that the titanium feedstock powder contains 0.13 wt.% oxygen and 0.014 wt.% nitrogen, which is in good agreement with the values given by the supplier. Hardness is determined to of 207 ± 6 HV 0.01. Figure 5 shows a micrograph of a powder cross section and illustrates that the particles have regular spherical shapes. The spray powders are dense and show no internal porosity.

3.2 Influence of Increased Process Gas Temperatures

Figure 6 illustrates the influence of process gas temperature on the strength of the resulting coatings. With increasing the process gas temperature from 600 to 1000 °C, the TCT-strength rises from about 120 up to

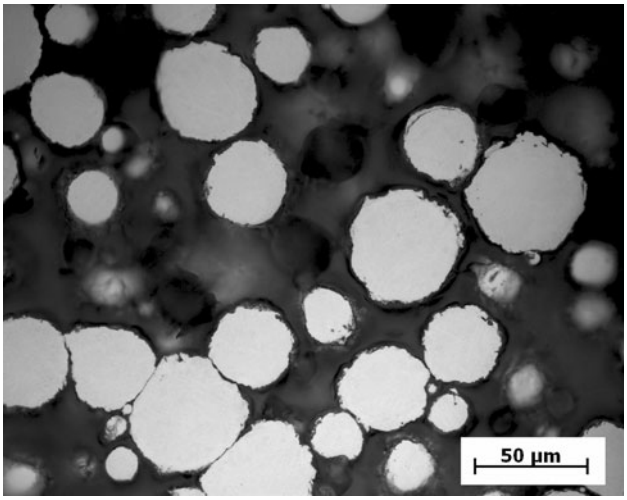

Fig. 5 Morphologies of the spherical Ti feedstock powder (OM micrograph of an as polished powder cross section)

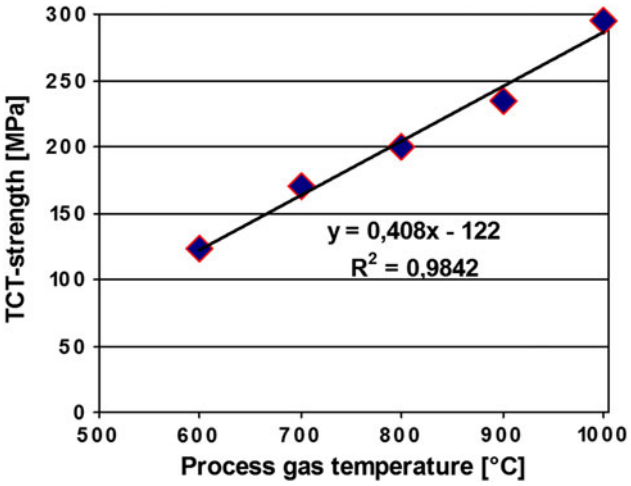

Fig. 6 TCT-strength for different process gas temperatures (gas pressure = 4 MPa, impact angle = 90°). The black line indicates the trend for increasing process gas temperatures. R^2 stands for the Pearson's correlation coefficient. Please note that strength values have not been corrected for the notch effect during TCT-testing

nearly 300 MPa. Taking into account the notch factor of 1.5, the ultimate tensile strength varies in range from 180 to 450 MPa, the high-end value being similar to that of bulk grade 3 titanium.

This rise can be attributed to two factors. One is the higher kinetic energy of the particles at higher gas temperatures. At the throat of the nozzle, the gas reaches the speed of sound, which in ideal gases is directly proportional to the square root of temperature. Thus, particle acceleration is more efficient and consequently, impact velocities are higher. The second reason for the increase of coating strength is the higher ductility of the spray material at higher temperatures. Thus, the critical velocities to obtain shear instabilities are reduced (Ref 6). Both effects

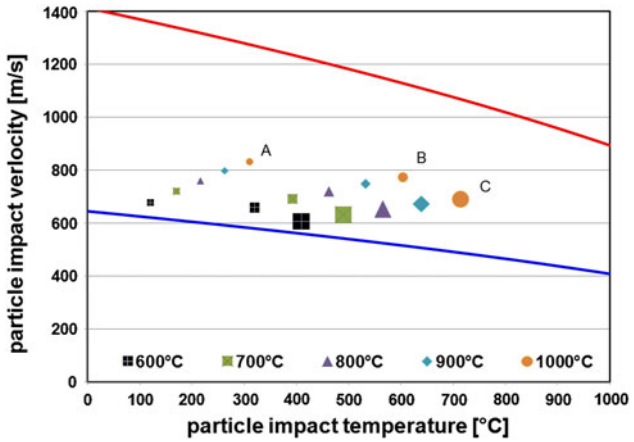

Fig. 7 Calculated Window of deposition for three different spherical particle sizes (diameter $A = 10$ µm, $B = 25$ µm, $C = 45$ µm) and nitrogen process gas temperatures between 600 and 1000 °C at 4 MPa of gas pressure. The lower line stands for the critical velocity, the upper red line for the erosion velocity

can be validated by comparing calculated impact conditions with critical velocities for bonding in a so called window of deposition (Fig. 7). The lower (blue) line corresponds to the critical velocity as defined for a deposition efficiency of 50% (Ref 6). For velocities smaller than the critical velocity, no or only very few particles will contribute to coating formation. The upper (red) line indicates velocities that could result in hydro-dynamic erosion. For coating formation, impact conditions should be met that are within the ''window of deposition'' as demarcated by these two lines (Ref 5). The isotropic fluid dynamic calculation of particle impact conditions demonstrates that particle temperatures and velocities are increased with process gas temperature. On the other hand, the critical velocities are decreased for higher temperatures.

In summary, particle impact velocities substantially exceed critical velocities. Consequently, areas that attain shear instabilities and concomitant heat generation increase (Ref 6). Therefore, nonbonded areas—the so-called south pole effect—diminish under harsher impact conditions (Ref 6). With a much larger amount of well-joined (welded) particle-particle interfaces, respective coatings show higher tensile strength than those obtained under lower process gas temperatures. These trends are confirmed by the powder impact morphologies as shown in Fig. 8. The morphologies shown in Fig. 8(a) are obtained by spraying under low parameter settings ($T = 600$ °C, $p = 4$ MPa). The particles are hardly deformed. Nevertheless, shear instabilities can be observed, but the ASI seem to be quite small. By increasing the process gas temperature to high-end parameter settings ($T = 1000$ °C, $p = 4$ MPa), the flattening ratio increases rapidly and shear instabilities appear to be more pronounced (Fig. 8b).

3.3 Influence of Spray Angles

Under ideal conditions as used to produce coatings for studying the influence of process gas temperatures on

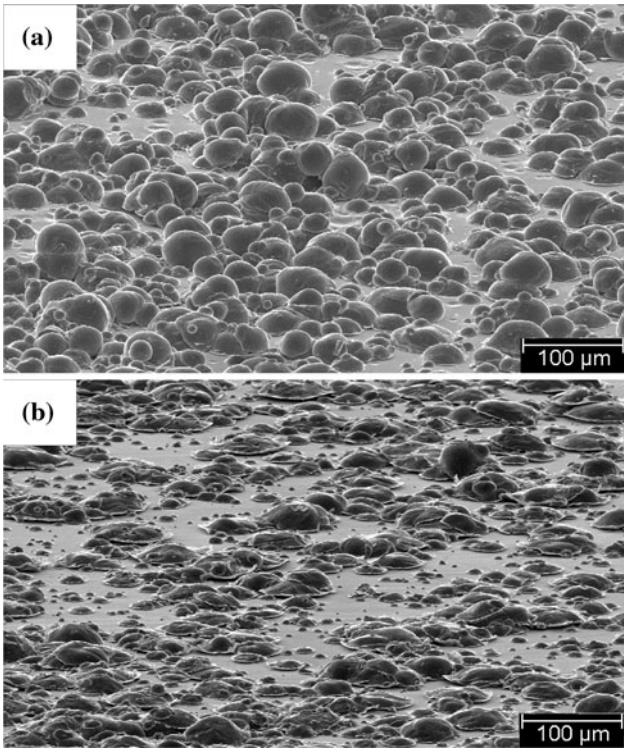

Fig. 8 Impact morphologies as obtained by wipe test with Ti particles sprayed under different conditions. The particles were sprayed at a nitrogen gas pressure of 4 MPa with $T_{gas} = 600$ °C (a) and with $T_{gas} = 1000$ °C (b). The spray angle was perpendicular

coating strength (Fig. 6), particles impact the substrate surface under perpendicular angle. For coating more complex shapes, these ideal conditions cannot be guaranteed for the whole part and coating quality might be reduced. Thus, in view of applications, the influence of impact angles on coating microstructures and properties has to be investigated. Figure 9 shows coatings microstructures obtained under optimum process gas parameters ($p = 4$ MPa, $T = 1000$ °C), but sprayed under different impact angles. As expected, perpendicular impacts (spray angle = 90°) lead to very dense and tight bonded microstructures (Fig. 9a). The porosity of 0.13% is negligible. By decreasing the spray angle—and thus increasing the deviation from ideal, perpendicular impacts—the porosity increases. Using an impact angle of 70° (Fig. 9b), the coating microstructure already shows more defects and an overall slightly higher porosity of 0.3% is determined. Further decreasing the impact angle down to 45° results in a columnar microstructure, reflecting the impact angle, with large, aligned pores (Fig. 9c), and a porosity of more than 6%.

The deformation characteristics for single impacts are shown in Fig. 10 for high-end parameter settings ($p = 4$ MPa, $T = 1000$ °C. For perpendicular spray angles (Fig. 10a), the impact morphologies reveal a high flattening ratio and distinct and large ASI symmetrically spread around each particle. Decreasing the impact angle down

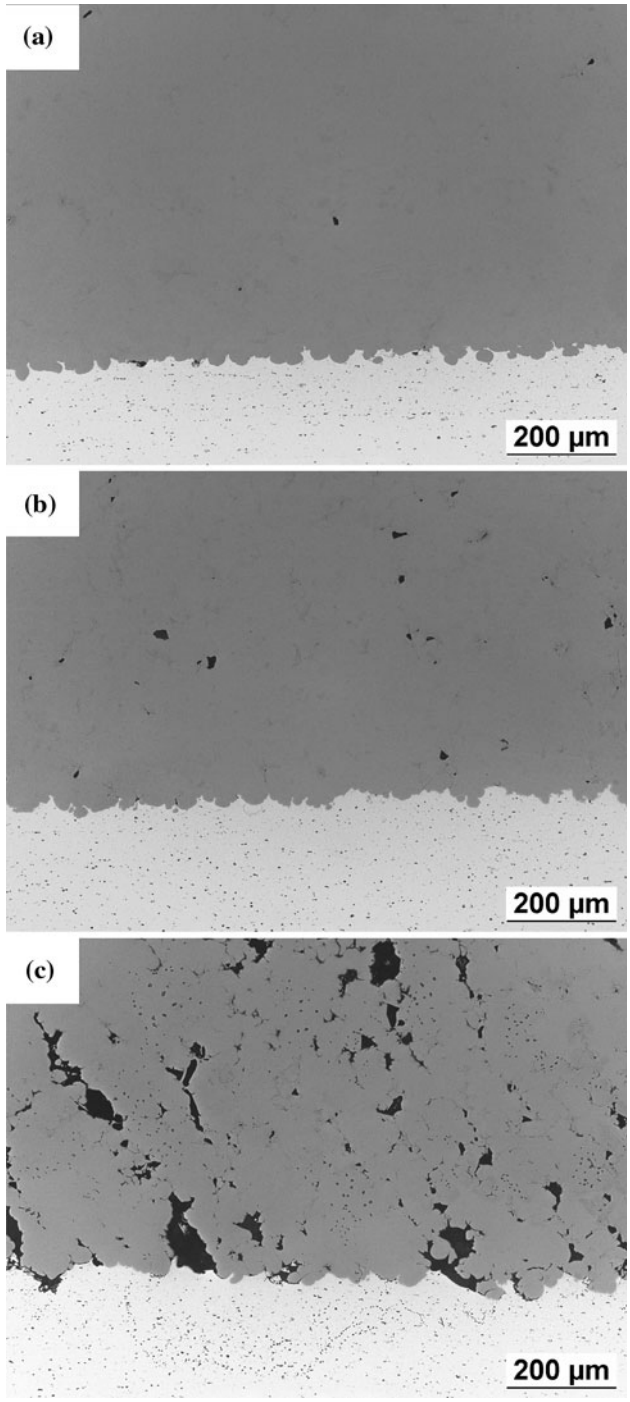

Fig. 9 Microstructures of cold sprayed Ti on $AlMg_3$-substrates for different spray angles, (a) 90°, (b) 70°, (c) 45°. The coatings were produced with nitrogen as process gas using a gas temperature of 1000 °C and a gas pressure of 4 MPa

to 85° has only minor influence on the flattening ratio and the extend of ASI (Fig. 10b). The impacts of the particles sprayed with an angle of 70° or below show a different behavior (Fig. 10c, d). The flattening ratio decreases and the ASI shifts. Thus, some of the flattened particles are only bonded on one side, while the other side has no

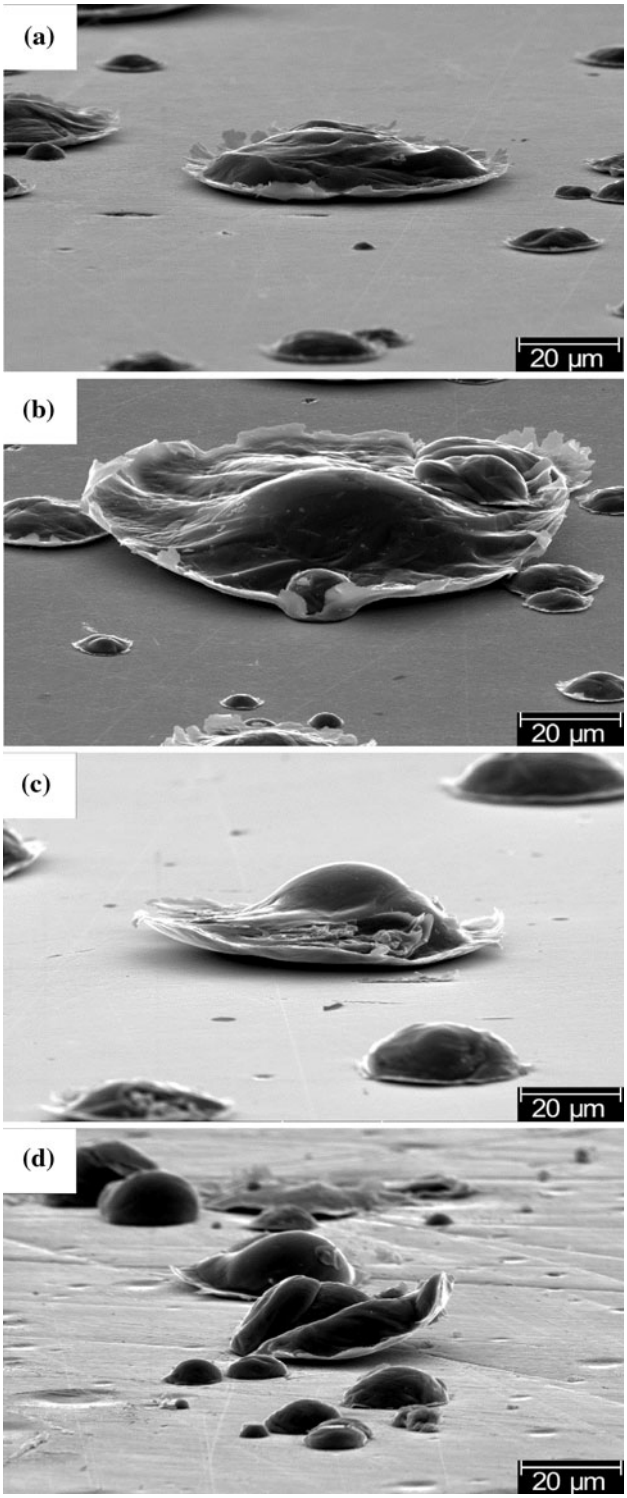

Fig. 10 Impact morphologies as obtained by wipe tests with Ti particles sprayed under different spray angles (a = 90°, b = 85°, c = 70°, d = 45°) on a polished low carbon steel sample by keeping the process gas temperature at 1000 °C and the pressure at 4 MPa. The flattening ratio is clearly decreasing by changing to lower spray angles

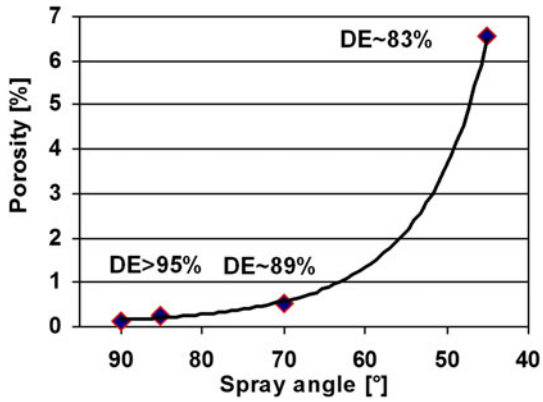

Fig. 11 Porosity of cold sprayed coatings for different spray angles. In addition, experimentally determined deposition efficiencies (DE) are indicated. Cold spraying was performed at a process gas temperature of 1000 °C and a gas pressure of 4 MPa. The black line indicates the trend of increase

contact to the substrate surface (Fig. 10d). Moreover, under lower impact angles the substrate surface shows more indents left by rebound particles (as visible in overviews, but not shown as separate figure).

Figure 11 shows the measured porosities versus the spray angle. The trend indicates that within a range of angles down to about 75°, porosity levels may be still tolerable. For flatter spray angles than 70°, the produced coatings show a steep increase in porosity. As also indicated in Fig. 11, the measured DE was quite high for all investigated spray angles, ranging from over 95% for perpendicular impacts, down to 83% for a spray angle of 45°.

3.4 Correlation of Spray Angles, Porosities with Shear Strength, and Coating Strengths

Figure 12 illustrates the influence of spray angle on the shear strength of titanium coatings for a process gas pressure of 4 MPa and different gas temperatures. For perpendicular spray angles, the shear strength can be increased from 70 to 81 MPa with process gas temperatures. For lower spray angles, the shear strength shows a roughly linear decrease with increasing deviation from ideal impacts, resulting in shear strengths in a range from 20 und 32 MPa for an impact angle of 45° and different process gas temperatures. Similar trends are well observed for coatings strengths (Fig. 13). Respective results show that TCT strength is reduced from about 290 MPa for perpendicular impacts down to about 90 MPa for a spray angle of 45° ($p = 4$ MPa, $T = 1000$ °C). For lower process gas temperatures, slightly lower strengths are obtained. The comparisons demonstrate that impact angles have more influence on coating properties than the investigated range of process gas temperatures. The correlation (Fig. 13) confirms that the amount of well-bonded particle-particle interfaces decreases with decreasing impact angles.

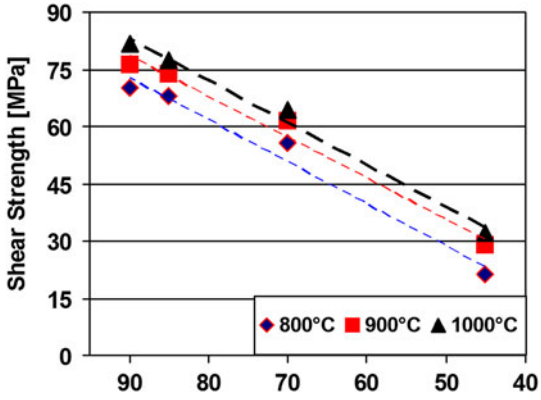

Fig. 12 Shear strength of cold sprayed Ti coatings on low carbon steel substrate for different spray angles and process gas temperatures. Cold spraying was performed at a gas pressure of 4 MPa. The dashed lines indicate the linearized trends of decrease

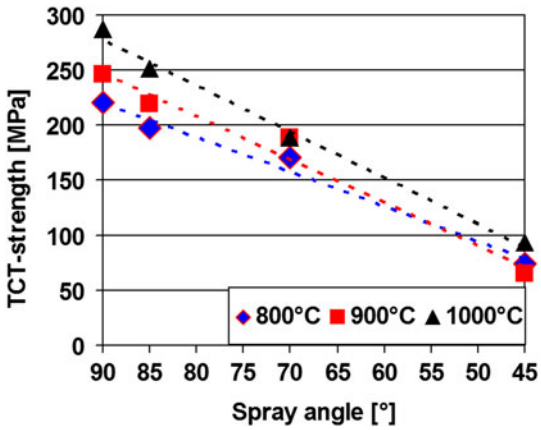

Fig. 13 TCT-strengths of cold sprayed titanium coatings for different spray angles and different nitrogen process gas temperatures. Cold spraying was performed at a gas pressure of 4 MPa. The dashed lines indicate the linearized trends of decrease

The decline in coatings strength for larger deviations from perpendicular impacts correlates well with the increase of coating porosities, both basing on drastic changes of impact conditions. As an example, Fig. 14 shows TCT-strengths versus coating porosity. Within a range of an increased porosity from roughly zero to about 1%, the tensile strength drops down from 287 MPa to nearly half. The decline of tensile coating strengths, as obtained in TCT-Tests, can be explained by the larger amount and larger sizes of remaining pores. More and larger pores act as crack nucleation centers, and decrease the material strength by supporting crack growth.

3.5 Effect of Impact Angle on Bonding

The description of nonperpendicular particle impacts has to consider several influences that have to be distinguished. First, a rotational momentum due to the velocity

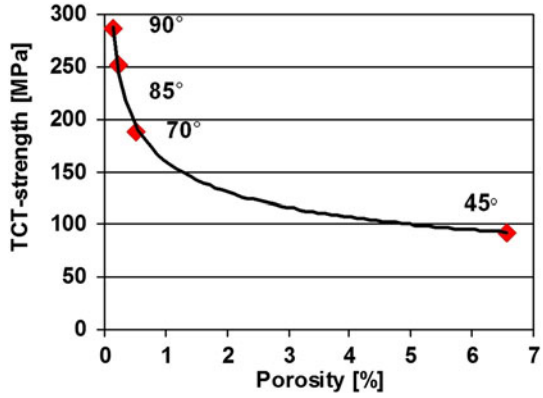

Fig. 14 Correlation between TCT-strength of Ti-coatings and porosity as obtained for different spray angles. The coatings were cold sprayed with nitrogen using a gas temperature of 1000 °C and a gas pressure of 4 MPa

component parallel to the substrate surface must be considered that may lead to detachment (compare Fig. 10d). With interfaces not being in contact, the larger amount of free volume cannot be closed by following particle impingements, resulting in an increasing porosity, as observed in Fig. 9(c).

Under increasing deviation from perpendicular impacts less plastic deformation but increasing heat generation by friction has to be considered (Ref 6). Modeling and SEM analyses (e.g., Fig. 10) of single impacts demonstrated that sites and ASI vary with decreasing impact angles imposing less deformation to the particle substrate interface, but—on the other hand—creating additional heat by friction (Ref 6). So far, it is not clear to which extend the heat generated by friction attributes to bonding, thus compensating lower heat generation by plastic deformation.

Previous investigations on the influence of spray angle for cold spraying copper with nitrogen or He as process gas (Ref 13, 14) showed that the deposition efficiency could be correlated to the impact angle. Under the high-end parameter settings of the present investigation for cold spraying fine titanium powders, the DE only declines by about 10% under a deviation of 45° from perpendicular impacts. Even at such flat impact angles, the particles still have enough kinetic and thermal energy to provide shear instabilities for bonding. For larger particle sizes, the larger rotational momentum might attribute to particle detachment.

In the previous investigations, it was suggested to correlate bonding and the DE under angular spray angle to the perpendicular component of the impact velocity (Ref 13, 14), which worked out for the cold spray parameter sets that operate at the steep increase of DE. However, for high-end parameters, the DE should be in a saturation regime and less sensitive for detecting differences in bonding mechanisms (Ref 6). A reliable analysis of the amount of bonded interfaces should be provided by investigating the mechanical coating properties as the shear strength or the TCT strength to elucidate influences by plastic deformation and heat of

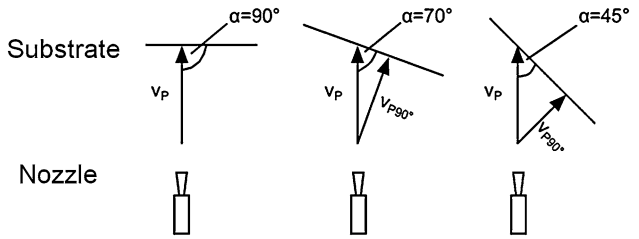

Fig. 15 Scheme for the velocity vectors for two dimensions. VP is the impact velocity vector along the spray jet, whereas $V_{P90°}$ corresponds to the part perpendicular to the substrate. "α" stands for the spray angle

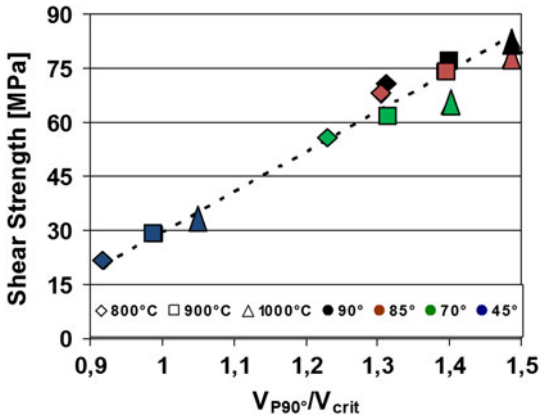

Fig. 16 Shear strength versus the characteristic factor out of perpendicular velocity vector divided by the critical velocity. The different colors (grey scales) symbolize the different spray angles. The dashed black line indicates the linearized trend

friction. Thus, as sketched in Fig. 15, an approach is followed to distinguish impact conditions in vector-terms of perpendicular velocities $V_{P90°} = v_p \sin \alpha$, with α as spray angle and v_p as particle velocity. Following the suggestion of Assadi (Ref 15), the excess with respect to the critical velocity is expressed as ratio between particle and critical velocities. Figure 16 and 17 shows respective plots for the shear strength and the TCT-strength. Both, the adhesive (shear) and the cohesive (TCT) strength can be correlated with the excess ratio of angular impact velocities with respect to critical velocities. The slight decrease in slope for high velocity ratios might be attributed to conditions reaching the saturation limit of strength, means similar properties as the respective bulk material. From this correlation it can be concluded that shear instabilities and heat generation to form bonded interfaces is mainly attributed to plastic deformation and only to minor amounts to heat generation by friction. It might be worth noting that even under perpendicular spray angle not necessarily all particles will hit the substrate under ideal conditions. Some (very small) particles might deviate from perpendicular impact angle by following the gas stream in the bow shock in front of the substrate, others might be subject to collisions.

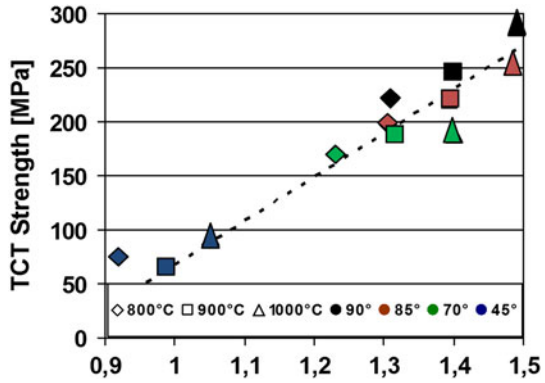

Fig. 17 TCT strength versus the characteristic factor out of perpendicular velocity vector divided by the critical velocity. The different colors (grey scales) symbolize the different spray angles. The dashed black line indicates the linearized trend

So far, these results just reveal trends. A detailed description of the correlation needs a statistically more sound data basis, which will be supplied by further spray experiments. In addition, further investigations will also concentrate on analyzing defects in more detail by working out correlations for the electrical conductivity as a measure for possible electron scattering sites.

The discussed effects should be transferable to cold spraying of other materials and impact conditions. However, the respective extent might vary depending on the mechanical properties of the spray material as well as the density and respective rotational momentum.

4. Summary and Conclusions

This study demonstrates that cold spraying of titanium coatings under high-end parameters using nitrogen as process gas at a pressure of 4 MPa and a temperature of 1000 °C results in ultimate strengths of about 450 MPa, similar to those of pure bulk material. For coating of complex geometries or building up bulk components, a deviation from the perpendicular spray angle will be inevitable and can locally decrease the mechanical properties. The analysis of different impact angles reveals that deviations from perpendicular impact conditions leads to increased porosity and decreased tensile and bonding strength of the coatings. However, if deviations from perpendicular impacts remain in a range of less than 20°, i.e., spray angle of 70° instead of 90°, coating strengths still reach 2/3 of the maximum values, which may be tolerable for quite a number of applications. The decline in coating strength with increasing deviation from perpendicular impact angle can be correlated with lower perpendicular excess velocity ratios with respect to critical velocities. The clear trends reveal that bonding is most prominently caused by shear instabilities under plastic deformation and only to minor extent by the heat of friction.

Acknowledgments

The authors would like to thank the laboratory staff, in alphabetical order, Thomas Breckwoldt, Herbert Hübner, Dieter Müller, Norbert Németh, Camilla Schulze, Matthias Schulze, and Uwe Wagener, for their support in this study.

References

1. "ASM Handbook Vol. 2, Properties and Selection: Nonferrous Alloys and Special-Purpose Materials," 10th ed., ASM International, Materials Park, 1992, p 610-614
2. Website Key to Metals http://nonferrous.keytometals.com/default.aspx?ID=CheckArticle&NM=165, Date of download 11.01.10
3. "ASM Metals Handbook Vol. 14: Forming and Forging," 9th ed., ASM International, Materials Park, 1988, p 594
4. H. Assadi, F. Gartner, T. Stoltenhoff, and H. Kreye, Bonding Mechanism in Cold Gas Spraying, *Acta Mater.*, 2003, **51**, p 4379-4394
5. T. Schmidt, F. Gartner, H. Assadi, and H. Kreye, Development of a Generalized Parameter Window for Cold Spray Deposition, *Acta Mater.*, 2006, **54**, p 729-742
6. T. Schmidt, H. Assadi, F. Gartner, H. Richter, T. Stoltenhoff, H. Kreye, and T. Klassen, From Particle Acceleration to Impact and Bonding in Cold Spraying, *J. Thermal Spray Technol.*, 2009, **18**, p 794-808
7. H. Wang, B. Hou, J. Wang, Q. Wang, and W. Li, Effect of Process Conditions on Microstructure and Corrosion Resistance of Cold-Sprayed Ti Coatings, *J. Thermal Spray Technol.*, 2008, **17**, p 738-739
8. G. Bae, S. Kumar, S. Yoon, K. Kang, H. Na, H. Kim, and C. Lee, Bonding Features and Associated Mechanisms in Kinetic Sprayed Titanium Coatings, *Acta Mater.*, 2009, **57**, p 5659-5660
9. S. Zahiri, C. Antonio, and M. Jahedi, Elimination of Porosity in Directly Fabricated Titanium via Cold Gas Dynamic Spraying, *J. Mater. Process. Technol.*, 2009, **209**, p 927
10. W. Wong, A. Rezaeian, S. Yue, E. Irissou, and J. Legoux, Effects of Gas Temperature, Gas Pressure, and Particle Characteristics on Cold Sprayed Pure Titanium Coatings, *Proc. International Thermal Spray Conference ITSC* 2009, B. Marple, M. Hyland, Y. Lau, C. Li, R. Lima, G. Montavon, Ed., 2009, p 233-234
11. G. Bae, K. Kang, H. Na, C. Lee, and H. Kim, Thermally Enhanced Kinetic Sprayed Titanium Coating: Microstructure and Property Improvement for Potential Applications, *Proc. International Thermal Spray Conference ITSC* 2009, B. Marple, M. Hyland, Y. Lau, C. Li, R. Lima, G. Montavon, Ed., 2009, p 293-294
12. S. Zahiri, D. Fraser, and M. Jahedi, Recrystallization of Cold Spray-Fabricated CP Titanium Structures, *J. Thermal Spray Technol.*, 2009, **18**, p 20-21
13. C.-J. Li and W.Y. Li, Examination of the Critical Velocity for Deposition of Particles in Cold Spraying, *Proc. International Spray Conference ITSC* 2005, Lugscheider E., Ed., DVS-German Welding Society, Düsseldorf, Germany, 2005 p 217-224 (on CD)
14. D.L. Gilmore, R.C. Dykhuizen, R.A. Neiser, T.J. Roemer, and M.F. Smith, Particle Velocity and Deposition Efficiency in the Cold Spray Process, *J. Thermal Spray Technol.*, 1999, **8**, p 576-582
15. H. Assadi, Parameter Selection in Cold Gas Spraying, *J. Thermal Spray*, in preparation
16. T. Schmidt, F. Gartner, and H. Kreye, New Developments in Cold Spray Based on Higher Gas- and Particle Temperatures, *J. Thermal Spray Technol.*, 2006, **4**, p 488-494